Eur. Phys. J. D **5**, 53–57 (1999)

THE EUROPEAN PHYSICAL JOURNAL D

EDP Sciences

Ultraviolet spectra of Mg in liquid helium

Y. Moriwaki[a] and N. Morita

Department of Molecular Structure, Institute for Molecular Science, Myodaiji, Okazaki 444-8585, Japan

Received: 1st July 1998 / Revised: 31 August 1998 / Accepted: 8 September 1998

Abstract. Emission and absorption spectra of Mg atoms implanted in liquid helium have been observed in the ultraviolet region. We have presented a model of exciplex formation of Mg–He_{10} and found that this model is more suitable for understanding the dynamics in the $3s3p\,^1P \rightarrow 3s^2\,^1S$ transition than the bubble model.

PACS. 32.30.Jc Visible and ultraviolet spectra – 36.40.Mr Spectroscopy and geometrical structure of clusters – 67.40.Yv Impurities and other defects

In the past decade, spectroscopic studies on foreign atoms in liquid helium have greatly been developed. This is mainly because of the interest in static and dynamical behaviors of the foreign atom itself, but it is also attractive that those studies are expected to give us useful information on the physical property of superfluid helium [1].

A foreign atom in liquid helium usually resides in a bubble-like cavity formed by Pauli's repulsive force between electrons in the foreign atom and in helium atoms. Large blue shift and broad linewidth in absorption spectra and small shift and narrow linewidth in emission spectra are characteristic properties of the foreign atom confined in a bubble, and these are well-understood on the basis of the bubble model [2], which assumes a bubble with a smooth and continuous atom-bubble interface. On the other hand, in some atoms, such as heavier atoms having a single valence electron (Rb, Cs and Ag), their $D2$ emission spectra are significantly red shifted or weakened [3,4], and these are successfully explained by a model of exciplex formation of He–X–He (X = Rb, Cs, Ag). In this case, the atom-bubble interface is no longer smooth nor continuous, but a part of the surrounding helium atoms are closely coupled with the foreign atom. For lighter alkali metal atoms (Li, Na and K), emission spectra have never been observed so far [5,6]. A similar exciplex formation model has been proposed to explain the quenching of emission for those atoms, but this has not been verified experimentally yet [7,8]. As for alkali earth atoms, there have been several studies on Be, Mg, Ca, Sr and Ba [2,9–15]. Among them, the research on lighter alkali earth atoms is, in particular, interesting in regard to the comparison with lighter alkali metal atoms, for which no emission has been observed. However, for lighter alkali earth atoms, there have been only a few studies [11–14] yet, and therefore it is quite desirable to advance the investigation on those atoms.

[a] e-mail: moriwaki@ims.ac.jp

Under these backgrounds, in the present work, we have observed absorption and emission spectra of Mg atoms in liquid helium by means of ultraviolet laser excitation. Two transitions have been observed and, in particular, a broad and significantly shifted emission line assigned to the $3s3p\,^1P \rightarrow 3s^2\,^1S$ transition has successfully been explained by an exciplex formation model. In this paper, we report these results and analysis in brief.

We adopt the ordinary implantation technique: Mg atoms are implanted by sputtering a small piece of Mg metal block placed in liquid helium with a second harmonic pulse (2 mJ) of a YAG laser followed by a 0.1 ms-delayed third harmonic pulse (2 mJ) of another YAG laser. The implanted atoms are excited with a second harmonic pulse of a Rhodamine 560 dye laser pumped by a third YAG laser. The laser induced fluorescence (LIF) from the Mg atoms is introduced into a 25 cm monochromator and is detected with a photo-multiplier. The temperature of the liquid helium is about 1.4 K.

The laser excitation scheme is shown in Figure 1. Examples of the observed spectra are shown in Figures 2 and 3, and their spectral properties are summarized in Table 1. In the present experiment, an emission

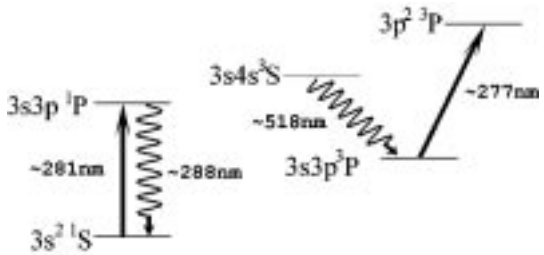

Fig. 1. Schematic diagram of laser excitation (straight arrows), fluorescence (waved arrows), and relevant energy levels of Mg atom in liquid helium.

Table 1. Experimental and theoretical spectral properties observed for Mg atom in liquid helium; λ_p (in nm) and $\Delta\lambda$ (in nm) are the peak wavelength and linewidth (in FWHM) of each spectrum, respectively.

free atom		experiment		bubble model*		exciplex model	
Transition	λ_0	λ_p	$\Delta\lambda$	λ_p	$\Delta\lambda$	λ_p	$\Delta\lambda$
$3s^2\,{}^1S \rightarrow 3s3p^1P$	285.2	281.5 ± 0.5	6.5 ± 0.5	278.3	9.0		
$3s^2\,{}^1S \leftarrow 3s3p^1P$	285.2	288.4 ± 0.2	3.2 ± 0.2	286.1	1.1	287.8	1.8
$3s3p^3P \rightarrow 3p^2\,{}^3P$	278 (six lines)	276.8 ± 0.5	3.7 ± 0.5				

* Ref. [15].

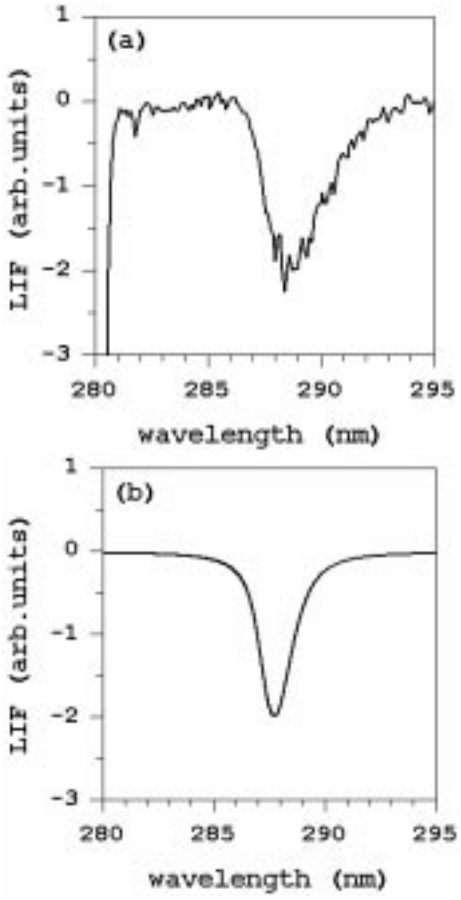

Fig. 2. Emission spectrum of Mg $3s^2\,{}^1S \leftarrow 3s3p\,{}^1P$. (a) Experimental spectrum observed by means of laser excitation at 280 nm. (b) Theoretical result calculated based on a model of Mg–He_{10} exciplex formation.

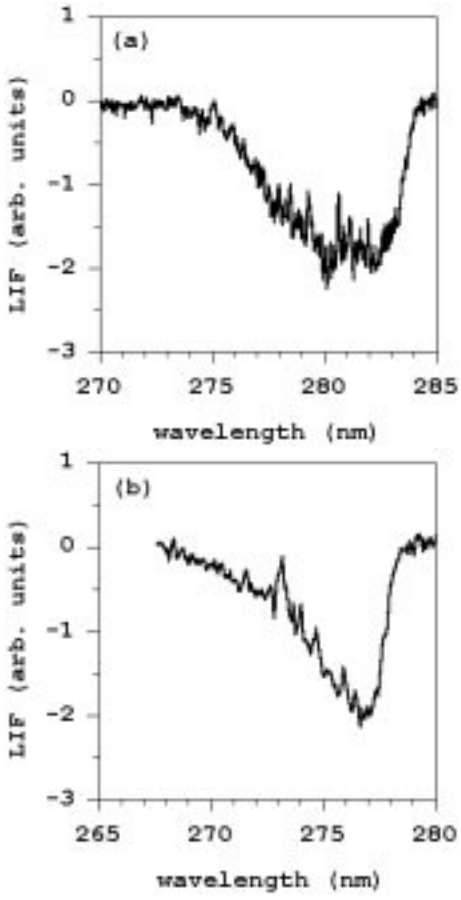

Fig. 3. (a) Excitation spectrum of $3s^2\,{}^1S \leftarrow 3s3p\,{}^1P$ observed by monitoring at 288 nm. (b) Excitation spectrum of $3s3p\,{}^3P \leftarrow 3p^2\,{}^3P$ observed by monitoring at 518 nm.

spectrum and an excitation spectrum are obtained with a laser pumping around 281 nm, and an excitation spectrum is obtained with a pumping around 277 nm. The former emission and excitation spectra, obtained by detecting LIF at 288 nm, are both assigned to the transitions between $3s3p\,{}^1P$ and $3s^2\,{}^1S$. On the other hand, the latter excitation spectrum, obtained by detecting LIF at 518 nm, is tentatively assigned to the $3s3p\,{}^3S \rightarrow 3p^2\,{}^3P$ transition, although there is still ambiguity. We will discuss this spectrum later.

In Table 1, we also show theoretical results [15] calculated for transitions between $3s^2\,{}^1S$ and $3s3p^1P$ on the basis of the bubble model. The bubble model is based on the following assumptions: the liquid helium is described as a continuous medium with a smooth density profile $\rho = \rho_0[1 - \{1 + \alpha(r - r_0)\}\exp\{-\alpha(r - r_0)\}]$, for $r > r_0$ and $\rho = 0$, for $r < r_0$, where ρ_0 is the bulk density of the liquid helium, and r_0 and α are variational parameters describing the size of the bubble and the slope of the bubble interface, respectively. The radius and shape of the bubble are determined so as to minimize the total energy, which consists of the interaction potential between the foreign atom and helium atom, the volume-pressure energy, and the surface energy of the liquid helium. As seen in Table 1, while the calculated results for the absorption

spectrum are in good agreement with the experimental values, the calculated wavelength shift and width of the emission spectrum are much smaller than the experimental results. This fact indicates that the bubble model underestimates the perturbation energy of the valence electrons in the lower state ($3s^2\,{}^1S$) by surrounding helium atoms.

It is reasonable to consider that the above underestimation results from a basic assumption in the bubble model; that is, in this model a bubble keeps its smooth shape before and after the transition of the foreign atom. As discussed in previous literature [3,4], the bubble model assuming a smooth helium density profile does not give a proper model calculation for states with attractive pair potentials, such as the ${}^2\Pi$ state of Rb–He, Cs–He, and Ag–He. The depth of the Mg–He pair potential in the ${}^1\Pi(3s3p)$ state (~ 42 cm^{-1} [16]) is larger than the heat of vaporization per single helium atom (~ 7.5 cm^{-1}), so that here we assume the formation of Mg–He$_n$ exciplex in which the helium atoms form a ring in the nodal plane of the $3p$ electron of the Mg atom.

The potential energy of this system is written as

$$U = \sum U_{\text{Mg}-\text{He}} + \sum U_{\text{He}-\text{He}} + \sum U_{\text{He}-bubble}, \quad (1)$$

where $U_{\text{Mg}-\text{He}}$ and $U_{\text{He}-\text{He}}$ are the Mg–He pair potential and the He–He pair potential, respectively, and $U_{\text{He}-bubble}$ is the interaction potential between the helium atom and bubble, described by

$$U_{\text{He}-bubble}(\mathbf{r}_i) = \int d^3r U_{\text{He-He}}(\mathbf{r}_i - \mathbf{r})\rho(\mathbf{r}), \quad (2)$$

where $\mathbf{r}_i$ is the position of the ith-helium atom in the ring. Using theoretical data [17–19], minimization of the total energy with respect to the number of helium atoms composing a ring gives a most probable exciplex Mg–He$_{10}$ in the ${}^1\Pi$ state with a total potential depth of $E = 503$ cm^{-1}.

To obtain a spectral profile for the transition from ${}^1\Pi(3s3p)$ to $\text{X}^1\Sigma(3s^2)$, we calculate the Franck-Condon factor by means of a spectral method, in which a spectrum is obtained by the Fourier transform of an autocorrelation function of wave functions with respect to the time evolution [20]. Here we assume that the vibration of the exciplex relaxes in much shorter time than the life time (2 ns) of the $3s3p\,{}^1P$ state owing to the coupling with phonon modes of the bulk liquid helium, and also that the separation between each vibrational level is much larger than the liquid helium temperature. These assumptions allow us to consider only the ground vibrational state. The dependence of the Mg–He pair potential on θ angle (in the polar coordinates) is shown in Figure 4. As can be seen from Figure 4, the initial wave function is expected to be confined in a small region of θ-angle. Since the ring is composed of ten helium atoms, the initial wave function is also restricted in a range within $\pi/5$ in ϕ angle. This confinement of the wave function within a small solid angle causes a large spread in the angular momentum space. We solve the wave function of the helium atom under the first order approximation that the angular-momentum-dependent part

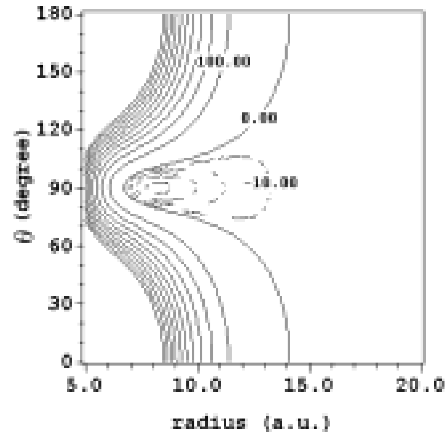

Fig. 4. The dependence of the Mg–He pair potential (in cm^{-1}) in the ${}^1\Pi$ ($3s3p$) state on the radius (r) and angle (θ) [16].

($V(\theta,\phi)$) of the potential is represented by angular variables at $r = r_m$, where the radial wave function is maximum with respect to θ angle, and that $V(\theta,\phi)$ is given by a square well potential for ϕ angle

$$V(\theta,\phi)=\begin{cases} 2mr_m^2/\hbar^2\left(U_{\text{Mg}-\text{He}}(r_m,\theta)-U_{\text{Mg-He}}(r_m,\frac{\pi}{2})\right), & \text{for } 0<\phi<\frac{\pi}{5} \\ \infty, & \text{elsewhere} \end{cases} \quad (3)$$

where m is the reduced mass of Mg and He. Then the initial wave function $\psi_0(\mathbf{r})$ is written in the form

$$\psi_0(\mathbf{r}) = R(r)\Theta(\theta)\Phi(\phi), \quad (4)$$

$$\left(\hat{l}^{\,2} + V(\theta,\phi)\right)\Theta(\theta)\Phi(\phi) = L^2\Theta(\theta)\Phi(\phi), \quad (5)$$

$$\left[-\frac{\hbar^2}{2m}\frac{1}{r^2}\frac{d}{dr}\left(r^2\frac{d}{dr}\right) + U(r) + \frac{\hbar^2}{2m}\frac{L^2}{r^2}\right]R(r) = ER(r), \quad (6)$$

where $\hat{l}$ is the angular momentum operator, L^2 and E are eigen values corresponding to the square of the angular momentum and energy, respectively. These eigen values are calculated to be $L^2 = 84.6$ and $E = -18.3$ cm^{-1} with $r_m = 9$ a.u. for the zero vibrational state. The energy of the first excited vibrational state is also calculated to be -7.1 cm^{-1}, and this means that the excitation energy of the first vibrational state is 11.2 cm^{-1}, which is much larger than the liquid helium temperature. This result is consistent with our assumption mentioned before.

After the transition to the $\text{X}^1\Sigma$ state, because the Mg–He pair potential is bound free and spherical, the helium atoms composing the ring rapidly diffuse in all directions. The effect of hard core parts in the He–He pair potential is negligibly small, so that we neglect the He–He

potential ($U_{\mathrm{He-He}}$). Then the angular momentum is conserved and the time evolution of the wave function $\psi(\mathbf{r},t)$ is given as

$$\psi(\mathbf{r},t)=\sum_{l,m}a_{lm}R_l(r,t)Y_{lm}(\theta,\phi), \tag{7}$$

$$i\hbar\frac{\partial}{\partial t}R_l(r)= \left[-\frac{\hbar^2}{2m}\frac{1}{r^2}\frac{d}{dr}\left(r^2\frac{d}{dr}\right)+U(r)+\frac{\hbar^2}{2m}\frac{l(l+1)}{r^2}\right]R_l(r), \tag{8}$$

where

$$a_{lm}=\int d\Omega Y^*_{lm}(\theta,\phi)\Theta(\theta)\Phi(\phi), \tag{9}$$

and $\mathrm{Y}_{lm}(\theta,\phi)$'s are spherical harmonics. The autocorrelation function is given by

$$\langle\psi_0(\mathbf{r})\mid\psi(\mathbf{r},t)\rangle=\sum_{l,m}\mid a_{lm}\mid^2\langle R(r)\mid R_l(r,t)\rangle. \tag{10}$$

There is no correlation between helium atoms in the zero point vibration, so that the spectrum of the system is given by

$$\int dt\,\{\langle\psi_0(\mathbf{r})\mid\psi(\mathbf{r},t)\rangle\}^{10}\exp(iEt). \tag{11}$$

The results of this calculation are shown in Table 1 and Figure 2. As seen in Table 1, the peak wavelength thus calculated is much closer to the experimental result than the value obtained on the basis of the bubble model, and considerable improvement is also seen with regard to the spectral broadening. This fact, we believe, means that the exciplex model is more suitable for understanding the dynamics in the $3s^2\,{}^1S\rightarrow 3s3p\,{}^1P$ transition than the bubble model.

We finally discuss another excitation spectrum observed in the present experiment. This excitation spectrum is obtained by detecting LIF at 518 nm for a laser pumping around 277 nm (for the same excitation wavelength, some fluorescence is seen at 288 nm as well, but it is difficult to obtain any excitation spectrum with this emission band because of its weakness and spectral overlapping with an emission due to the excitation of $3s^2\,{}^1S\rightarrow 3s3p\,{}^1P$). Although the 518 nm fluorescence corresponds to the $3s4s\,{}^3S\rightarrow 3s3p\,{}^3P$ transition, it is more reasonable to consider that the observed spectrum is an excitation spectrum of the $3s3p\,{}^3P\rightarrow 3p^2\,{}^3P$ transition (see Fig. 1). It is because this assignment allows us to understand the small shift and broadening of the spectrum: *i.e.* the size of the $3p$ electron in the $3p^2\,{}^3P$ state is smaller than in the $3s3p\,{}^1P$ state because of a smaller shielding effect for the core charge by the rest of valence electrons. Therefore, we can consider that the perturbation energy of the valence electron by surrounding helium atoms is smaller when the $3p^2\,{}^3P$ state is excited from the $3s3p\,{}^3P$ state than when $3s3p\,{}^1P$ is excited from $3s^2\,{}^1S$ (see Fig. 3).

For the $3p^2\,{}^3P$ state, there is no calculation for the Mg–He pair potential because of the complexity of closely lying electric states. However, a very approximate form of the potential can be estimated to be $V=\sin^2\theta V_\sigma+(1+\cos^2\theta)V_\pi$, where V_σ and V_π are interaction potentials between the $3p$ electron and He [7]. Therefore, the formation of He–Mg–He exciplex is expected to minimize the total energy in the $3p^2\,{}^3P$ state. In this case, an emission spectrum with a large red shift and broad linewidth is expected to be observed just like the case of the $5p\,{}^2P_{3/2}\rightarrow 5s\,{}^2S_{1/2}$ transition in Ag [3] and the $5p^2\,{}^3P\rightarrow 5s5p\,{}^3P$ transition in Sr [14]. But no emission band other than 518 nm and 288 nm is observed in a wavelength region between 270 nm and 650 nm for the pumping at the 277 nm band. The direct emission spectrum from $3p^2\,{}^3P$ to $3s3p\,{}^3P$ might overlap coincidentally with the $3s3p\,{}^1P\rightarrow 3s^2\,{}^1S$ emission spectrum, or some radiationless relaxation channel might exist. Such radiationless relaxation dynamics might be described as follows: (1) according to Hui *et al.* [14] and Takami [21], the ionization energy lowers by 1.8 eV in liquid helium in comparison with that of a free atom. This means that Mg atom in the $3p^2\,{}^3P$ state, which lies 0.5 eV below the ionization energy, ionizes in liquid helium. (2) The emitted electron forms an electron bubble, and Mg^+ ion in the $3p\,{}^2P$ state forms Mg^+–He_n exciplex in the ${}^2\Pi$ state. (3) This exciplex relaxes to a bound free ${}^2\Sigma$ state adiabatically without emission. (4) A succeeding recombination process results in the production of an excited Mg atom. At this point, the $3s3p\,{}^1P$ state as well as $3s4s\,{}^3S$ can be populated. (5) Then, finally, this Mg atom deexcites with emitting fluorescence at 288 nm and/or 518 nm. This is one of the possible mechanisms responsible for the absence of fluorescence in the $3s3p\,{}^3S\leftarrow 3p^2\,{}^3P$ transition and for the appearance of fluorescence, instead, in another transition. Moreover, the weak emission observed at 288 nm, mentioned before, might be caused by the above mechanism. However, it is still unknown whether this mechanism is true, and it is interesting future work to find out the correct mechanism.

In conclusion, we observed the $3s^2\,{}^1S\leftrightarrow 3s3p\,{}^1P$ and $3s3p\,{}^3P\rightarrow 3p^2\,{}^3P$ transition spectra of Mg in liquid helium. It was found that the large red shift and broadening in the observed emission spectrum are better understood by a model of Mg–He_{10} exciplex formation than by the bubble model. This result suggests that light alkali metal atoms might form the same type exciplexes in liquid helium.

References

1. Z. Phys. B **98**, No. 3 (1995), special issue on ions and atoms in superfluid helium.
2. S.I. Kanorsky, M. Arndt, R. Dziewior, A. Weis, T.W. Hänsch, Phys. Rev. B **50**, 6296 (1994).
3. J.L. Persson, Q. Hui, Z.J. Jakubek, M. Nakamura, M. Takami, Phys. Rev. Lett. **76**, 1501 (1996).
4. T. Kinoshita, K. Fukuda, T. Matsuura, T. Yabuzaki, Phys. Rev. A **53**, 4054 (1996).

5. Y. Takahashi, K. Sano, T. Kinoshita, T. Yabuzaki, Phys. Rev. Lett. **71**, 1035 (1993).
6. T. Yabuzaki (private communication); T. Yabuzaki *et al.* have very recently observed the D line emission from potasium atoms in an infrared region.
7. J. Dupont-Roc, Z. Phys. B **98**, 383 (1995).
8. S. Kanorsky, A. Weis, M. Arndt, R. Dziewior, T.W. Hänsch, Z. Phys. B **98**, 371 (1995).
9. H. Bauer, M. Beau, A. Bernhardt, B. Friedl, H.J. Reyher, Phys. Lett. A **137**, 217 (1989).
10. H. Bauer, M. Beau, B. Friedl, C. Marchand, K. Miltner, H.J. Reyher, Phys. Lett. A **146**, 134 (1990).
11. J.H.M. Beigersbergen, Q. Hui, M. Takami, Phys. Lett. A **181**, 393 (1993).
12. B. Tabbert, M. Beau, H. Günther, W. Häußler, C. Hönninger, K. Meyer, B. Plagemann, G. zu Pulitz, Z. Phys. B **97**, 425 (1995).
13. H. Günther, M. Foerste, C. Hönninger, G. zu Putlitz, B. Tabbert, Z. Phys. B **98**, 395 (1995).
14. Q. Hui, J.L. Persson, J.H.M. Beijersbergen, M. Takami, Z. Phys. B **98**, 353 (1995).
15. J.-Z. Tang, M. Kimura, I. Shimamura, Chem. Phys. Lett. **256**, 327 (1996).
16. M. Kimura, I. Shimamura (private communication).
17. E. Czuchaj, H. Stoll, H. Preuss, J. Phys. B **20**, 1487 (1987).
18. R.A. Aziz, M.J. Slaman, J. Chem. Phys. **94**, 8047 (1991).
19. E. Cheng, M.W. Cole, W.F. Saan, J. Treiner, Phys. Rev. Lett. **67**, 1007 (1991).
20. M.D. Feit, J.A. Fleck, A. Steiger, J. Comput. Phys. **47**, 412 (1982).
21. M. Takami, Comm. At. Mol. Phys. **32**, 219 (1996).